

Do evolved stars in the LMC show dual dust chemistry?

E. Marini,^{1,2★} F. Dell’Agli,^{3,4} D. A. García-Hernández,^{3,4} M. A. T. Groenewegen,⁵
S. Puccetti,⁶ P. Ventura² and E. Villaver⁷

¹*Dipartimento di Matematica e Fisica, Università degli Studi Roma Tre, via della Vasca Navale 84, I-00100 Roma, Italy*

²*INAF, Osservatorio Astronomico di Roma, Via Frascati 33, I-00077 Monte Porzio Catone, Italy*

³*Instituto de Astrofísica de Canarias (IAC), E-38200 La Laguna, Tenerife, Spain*

⁴*Departamento de Astrofísica, Universidad de La Laguna (ULL), E-38206 La Laguna, Tenerife, Spain*

⁵*Koninklijke Sterrenwacht van België, Ringlaan 3, B-1180 Brussels, Belgium*

⁶*ASI, Via del Politecnico, I-00133 Roma, Italy*

⁷*Departamento de Física Teórica, Universidad Autónoma de Madrid, Cantoblanco, E-28049 Madrid, Spain*

Accepted 2019 June 28. Received 2019 June 28; in original form 2019 May 6

ABSTRACT

We study a group of evolved M-stars in the Large Magellanic Cloud, characterized by a peculiar spectral energy distribution. While the 9.7 μm feature arises from silicate particles, the whole infrared data seem to suggest the presence of an additional featureless dust species. We propose that the circumstellar envelopes of these sources are characterized by a dual dust chemistry, with an internal region, harbouring carbonaceous particles, and an external zone, populated by silicate, iron, and alumina dust grains. Based on the comparison with results from stellar modelling that describe the dust formation process, we deduce that these stars descend from low-mass ($M < 2 M_{\odot}$) objects, formed 1–4 Gyr ago, currently evolving either in the post-AGB phase or through an after-pulse phase, when the shell CNO nuclear activity is temporarily extinguished. Possible observations able to confirm or disregard the present hypothesis are discussed.

Key words: stars: abundances – stars: AGB and post-AGB – Magellanic Clouds.

1 INTRODUCTION

The Large Magellanic Cloud (LMC) has been so far the most investigated environment to test asymptotic giant branch (AGB) evolution modelling, owing to its relative proximity (~ 50 kpc; Feast 1999) and low average reddening ($E(B - V) \sim 0.075$, Schlegel, Finkbeiner & Davis 1998).

The Surveying the Agents of a Galaxy’s Evolution Survey (SAGE, Meixner et al. 2006), with the *Spitzer Space Telescope*, provided mid-infrared (IR) data of millions of AGB stars, that allowed to study the dust enrichment from the individual sources (e.g. Srinivasan et al. 2009) and to estimate the current dust production rate by AGB stars in the LMC (Matsuura 2009; Schneider et al. 2014).

Among the results from the *Spitzer* space mission we stress the importance of the SAGE-Spec atlas (Kemper et al. 2010), obtained with the Infrared Spectrograph (IRS). The availability of the spectral energy distribution (SED) in the whole mid-IR region offers a valuable opportunity of determining the luminosity and the dust composition within the circumstellar envelope of the individual sources observed. The latest developments in AGB modelling,

with the evolution of the central star coupled to the description of dust formation in the wind, allow the characterization of the individual sources, in terms of the properties of the progenitors and the evolutionary phase (Dell’Agli et al. 2015a,b).

This research will be of paramount importance for the incoming James Webb Space Telescope (JWST) mission, because the analysis so far being limited to the Magellanic Clouds (MCs) can be extended to all the galaxies in the Local Group. The recent studies by Jones et al. (2014, 2017) are extremely important in this regard, as they provided the magnitudes of obscured M-stars in the LMC that would be found if they were observed with the JWST filters.

Against this background we decided to extend the analysis by Jones et al. (2014), using the results from AGB modelling to interpret the IRS SED and to characterize the individual sources. In a first study we focused on a few stars with a peculiar SED, which we interpreted as massive metal-poor AGB stars, whose dust composition is dominated by solid iron particles (Marini et al. 2019).

In this paper we focus on eight sources, which we propose to be characterized by a dual dust chemistry, surrounded by an internal dust layer and an external shell, populated, respectively, by carbonaceous particles and silicate grains.

The idea that AGB stars with dual chemistry exist was proposed independently by Willems & de Jong (1986) and Little-Marenin (1986), after the detection of objects that showed clear absorption

* E-mail: ester.marini@uniroma3.it

bands from carbon-rich molecules in their optical and near-IR spectra while showing silicate emission in the mid-IR. The possible presence of such systems is challenged by the expansion of the outer silicate-rich layer, to the point where the silicate feature is no longer detectable (Chan & Kwok 1988). On the other hand, the formation of a disc, possibly related to the presence of a companion, might prevent the escape of the external silicate shell (Lloyd Evans 1990). Here we try to identify the physical conditions and the evolutionary phases allowing the formation of this class of objects.

These findings will be also important to identify dual dust chemistry stars in samples of evolved stars in galaxies.

2 DUST FORMATION IN LOW-MASS AGB STARS

We used the AGB models discussed by Ventura et al. (2014), where the description of dust formation in the wind is coupled to the evolution of the central stars, i.e. the variation of the main physical properties (luminosity, effective temperature, mass-loss rate) and the surface chemical composition. In this work we use models with $Z = 8 \times 10^{-3}$, the dominant metallicity in the LMC (Harris & Zaritsky 2009) that were presented by Dell’Agli et al. (2014, 2015a,b). For the scope of this investigation, we extended the tracks of the stars of initial mass below $2 M_{\odot}$ to the post-AGB phase, up to effective temperatures $\sim 5 \times 10^4$ K (these results will be presented in a forthcoming paper).

Fig. 1 shows the AGB evolution of stars of initial mass $1.2 M_{\odot} \leq M \leq 2 M_{\odot}$, all reaching the C-star stage. We report the variation of the surface C/O ratio (left-hand panel), the luminosity (middle), and the excursion of the tracks in the HR diagram during the post-AGB phase (right).

The stars of mass below $2 M_{\odot}$ experience a last thermal pulse (TP), after which they become C-stars, then start the post-AGB evolution, without experiencing further TPs. This is because after the $C/O > 1$ condition is reached a significant increase in the rate of mass-loss speeds up the loss of the envelope (Lagadec & Zijlstra 2008), thus preventing additional TPs.

These stars produce oxygen-rich dust for most of their lives on the AGB, but the phases following the last TP, when they produce carbonaceous dust. The change in the dust mineralogy associated with the occurrence of the TP set the conditions for the presence of two dusty shells, with amorphous carbon and silicate dust. These results indicate that the hypothesis that a late TP converts an M-star into a C-star, proposed by Perea-Calderón et al. (2009) to explain the dual chemistry phenomenon in Galactic bulge planetary nebulae (hereafter PNe), is indeed a common behaviour of all the stars formed between 1 and 4 Gyr ago.

$M \geq 2 M_{\odot}$ behave differently, because they accumulate large quantities of carbon in the photosphere, that favour the formation of great quantities of carbonaceous dust (Lagadec & Zijlstra 2008; Dell’Agli et al. 2015a).

Fig. 1 shows that the luminosities experienced during the interpulse phase of the AGB life are in the range $3\text{--}10 \times 10^3 L_{\odot}$, while the C-star stage is reached when $5 \times 10^3 L_{\odot} < L < 10^4 L_{\odot}$. During the phases following the ignition of the TP, when the CNO nuclear activity in the shell is temporary extinguished, the luminosities drop to $\sim 2 \times 10^3 L_{\odot}$. The right-hand panel of Fig. 1 shows that the luminosities attained during the post-AGB phase are in the range $6 \times 10^3 L_{\odot} < L < 9 \times 10^3 L_{\odot}$, and stay approximately constant as the evolutionary tracks move to hotter effective temperatures. These results are consistent with the $Z = 0.01$ post-AGB models published by Miller Bertolami (2016).

3 DUAL DUST CHEMISTRY M-STARS

We consider the M-stars in the LMC with IRS spectra available, selected by Jones et al. (2014). To study the distribution of the observational planes we use the mid-IR magnitudes calculated by Jones et al. (2017), who integrated the SED of each source over the MIRI spectral response.

The left-hand panel of Fig. 2 shows the distribution of these stars in the colour–colour plane ($[7.7]\text{--}[25.5]$, $K_S - [7.7]$) (we expect to obtain similar trends when using the NIRCам F210M filter). The stars trace an obscuration sequence, up to colours $[7.7]\text{--}[25.5] \sim 3$ and $K_S - [7.7] \sim 6$. An obscuration path is also present in the colour–magnitude diagram ($K_S - [7.7]$, $[7.7]$) (see middle panel of Fig. 2).

The stars highlighted with colour symbols fall off the obscuration sequences. This is particularly evident in the middle panel, where these sources define a vertical sequence below the main obscuration pattern, at $K_S - [7.7] \sim 2.5\text{--}3.5$.

The peculiar position of these objects in the observational planes is due to their SED: while the $9.7 \mu\text{m}$ feature indicates the presence of silicates, the continuum in the $\lambda < 8 \mu\text{m}$ region suggests the presence of a featureless dust species. The two most plausible options are solid iron and amorphous carbon, given the low stability and the small abundances of other species. A dominant contribution from solid iron to the overall extinction was explored by Marini et al. (2019) in the context of low-metallicity, massive AGB stars, in which strong hot bottom burning (hereafter HBB) inhibits the formation of silicates, via the destruction of the surface oxygen and magnesium. This possibility can be ruled out in the present case, because the luminosities of the stars analysed here, below $10^4 L_{\odot}$, are much smaller than those typical of the stars undergoing HBB, above $2 \times 10^4 L_{\odot}$. Therefore, we will base our analysis on the hypothesis of the presence of a dust layer composed by amorphous carbon.

In the following we divide these stars into two groups, according to the morphology of their SED, derived from IRS and photometric data. This classification can be appreciated in the colour–colour diagram ($I - K_S$, $K_S - [7.7]$) shown in the right-hand panel of Fig. 2, in which these two groups clearly separate from each other.

3.1 A class of post-AGB stars

The sources plotted with blue open diamonds in Fig. 2 exhibit a short-wavelength peak, at $\sim 0.4\text{--}0.6 \mu\text{m}$, and two features, at 9.7 and $18 \mu\text{m}$, that reveal the presence of silicates. An example is shown in the right-hand panel of Fig. 3. This SED indicates a post-AGB nature, because the effective temperatures deduce from SED fitting are above ~ 5000 K.

We propose that these post-AGB stars descend from $1.2 \leq M/M_{\odot} < 2$ progenitors. A nice fit of the observed SED (see right-hand panel of Fig. 3) is obtained by assuming the presence of two dusty layers: the more internal is composed by carbon dust, whereas the more external hosts mainly silicate particles. A similar explanation was invoked by Bunzel et al. (2009) to interpret the SEDs of Galactic O-rich post-AGB stars (heavily obscured and showing strong silicate absorption) although their peculiar SEDs could be fitted with pure silicate dust when including very large and cold grains (R. Szczerba 2019, private communication); a possibility that we rule out for the significantly less obscured stars discussed here.

Based on the discussion in the previous section, we believe that the two dust layers formed just before and after the last TP, when the transition from M-star to C-star occurred. This interpretation is

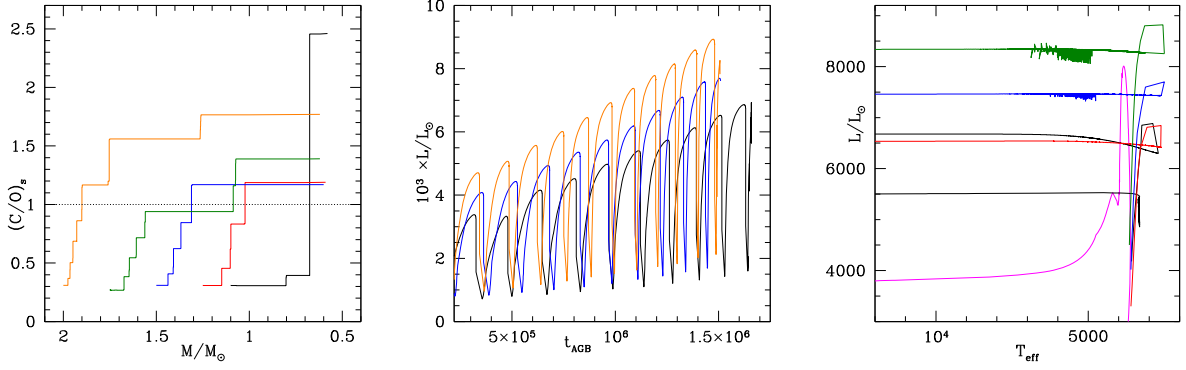


Figure 1. Left: the variation of the surface C/O ratio during the AGB evolution of stars of initial masses 1.2 (black line), 1.3 (red), 1.5 (blue), 1.75 (green), and 2 M_{\odot} (orange). Middle: the evolution of the luminosity of the 1.2, 1.5, and 2 M_{\odot} stars in the HR diagram. The pink line corresponds to a star of mass 1 M_{\odot} and the light lines on the right refer to the AGB phase and connect the temperatures and luminosities of the stars during the interulses.

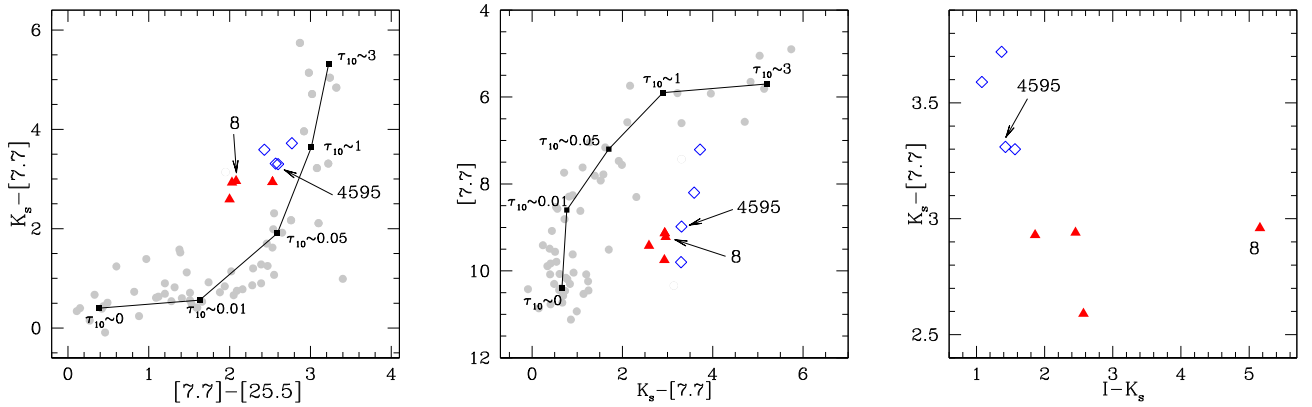


Figure 2. Distribution of the sample of M-stars in the LMC analysed by Jones et al. (2017), indicated by grey points, in the colour–colour (left-hand panel) and in the colour–magnitude diagrams (middle panel). Blue open diamonds and red full triangles indicate the two groups of stars discussed in this paper. The black lines indicate a theoretical obscuration sequence of M-stars, assuming a dust composition made up of silicates, alumina dust, and solid iron. Typical values of the optical depth at 10 μm and the position of the sources SSID 8 and SSID 4595 are indicated. In the right-hand panel is shown a diagram with a colours combination able to clearly separate the stars among the two groups described in sections 3.1 and 3.2 I magnitudes come from Zaritsky et al. (2004).

supported by the luminosities required to reproduce the SED, in the range $5\text{--}10 \times 10^3 L_{\odot}$, in agreement with the post-AGB luminosities reported in the right-hand panel of Fig. 1. This understanding is in agreement with the fact that only one source shows a 90-d period, and the other seven show no signs of variability (Jones et al. 2017). A further probe for this interpretation comes from the presence of a weak PAH-like emission feature at 6.3 μm in a post-AGB star in our sample (SSID 4547), confirming the presence of C-rich material and the classification as post-AGB stars¹.

The presence of these stars in the AGB sample is due to the criterion followed to distinguish AGB from post-AGB stars, discussed by Woods et al. (2011, see their fig. 3). Post-AGB stars are commonly identified by the presence of two distinct peaks in the SED, located in the $\lambda < 1 \mu\text{m}$ portion of the spectrum and at 9.7 μm , separated by a clear minimum in the SED at $\sim 2 \mu\text{m}$. The presence of carbon dust affects significantly the shape of the SED

in the 1–8 μm region, preventing the appearance of a minimum, making the SED very similar to an M-type AGB.

The Milky Way is known to host dual chemistry PNe (Gutenkunst et al. 2008; Guzman-Ramirez et al. 2011; García-Hernández & Górný 2014) and post-AGB stars (Waelkens et al. 1996; Molster et al. 2001; Cerrigone et al. 2009); however, no dual chemistry PNe or post-AGB stars have been previously detected in the MCs (Stanghellini et al. 2007; Bernard-Salas et al. 2009), which could pose a problem to the present suggestion of the existence of dual chemistry post-AGBs. However, this might be just a consequence of small-number statistics given the low number of PNe that has been observed in the MCs in the infrared compared with the number of AGBs stars.

3.2 Faint, dusty AGB stars

The SED of the stars indicated with red full triangles in Fig. 2 show evidence of cool dust, with a peak at 9.7 μm , revealing the presence of silicate grains. The left-hand panel of Fig. 3 shows an example of these spectra. The luminosities deduced from SED fitting fall in the range $2\text{--}4 \times 10^3 L_{\odot}$.

¹A few PNe with a similar dual dust chemistry (i.e. PAHs + amorphous silicates) have been observed in our Galaxy (e.g. Perea-Calderón et al. 2009). Curiously, their 6.3 μm feature is always the strongest one, as seen in our star SSID 4547.

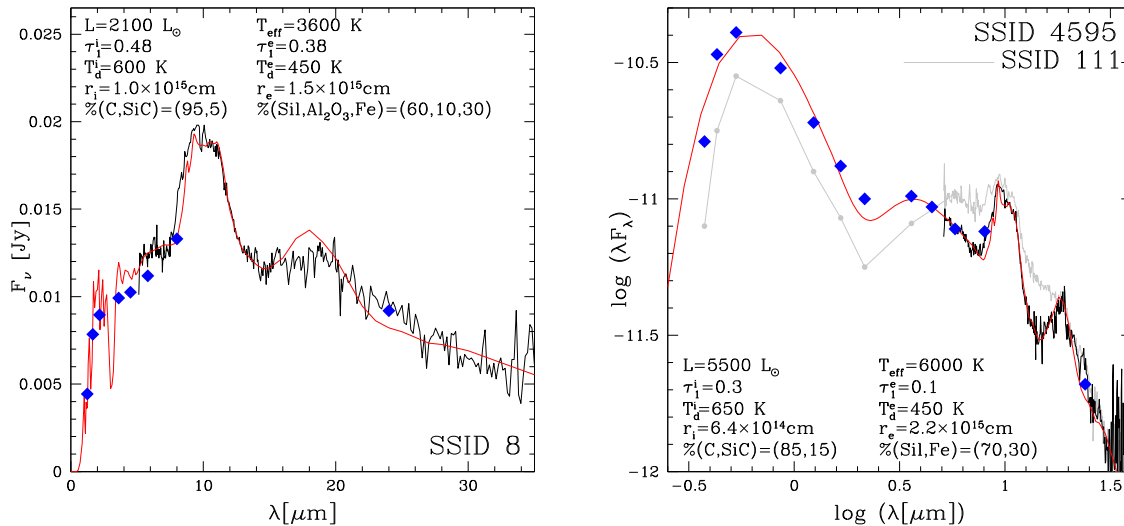


Figure 3. The comparison between the observed IRS spectra (in black) and the synthetic SED (in red) of the stars in the LMC sample by Woods et al. (2011): SSID 8 (left-hand panel, see Fig. 2) and SSID 4595 (right). Blue diamonds show *Spitzer* photometry from Meixner et al. (2006) and optical + near IR data, available in the literature. The grey line in the right-hand panel refers to SSID 111, classified as a post-AGB stars from Woods et al. (2011). In both panels we report the luminosity and effective temperature of the star, and the following parameters for the internal and outer dust shells: optical depth (at 1 μm), dust temperature, dust composition, and distance from the central star. For SSID 8 we modelled the emission from the central star with a GRAMS atmosphere corresponding to the best-fitting effective temperature, while for SSID 4595 we used a blackbody spectrum.

Obscured M-stars are produced either from $M > 3 M_{\odot}$ stars experiencing HBB or to low-mass stars (initial masses below $\sim 1.5 M_{\odot}$) evolving through advanced AGB phases, before becoming carbon stars. Both explanations are not plausible in this case, because the luminosities would be much in excess of those observed. Furthermore, we have not found a way of reproducing the SED in the 4–8 μm region, without assuming significant amounts of carbon dust.

As discussed in the previous section (see middle panel of Fig. 1), the luminosities given above are compatible with the post-TP phases of low-mass stars. During these phases dust formation stops, because the drop in the mass-loss rate provokes a significant decrease in the density of gaseous particles available to condensation.

We propose that these stars have reached the C-star stage via a TDU episode that followed the previous TP, and are currently evolving through a post-TP, low-luminosity phase. Similarly to the post-AGB stars discussed earlier in this section, we reproduce their SED by two dusty layers, with a more internal zone, populated by carbonaceous particles, and an outer region, with silicate grains. As shown in the left-hand panel of Fig. 3, the synthetic SED obtained with these assumptions reproduces the IRS and photometric data well. Both dusty layers are cool, in agreement with the expectation that dust formation is halted during these low-luminosity phases. The source shown in the left-hand panel of Fig. 3 was studied by Groenewegen & Sloan (2018), who tried to fit its SED by adopting a single silicate dust shell. As shown in the two bottom left panels on page 77 of that paper, some significant differences between the observed SED and the best fitting exist. The dual chemistry model, compared to the single silicate dust shell, agrees better, particularly in the location of the primary peak and in the flux in the $\lambda > 15 \mu\text{m}$ domain.

4 DISCUSSION

According to our interpretation the two groups of stars discussed here have a common origin, as all of them descend from progenitors of mass $1 M_{\odot} < M < 2 M_{\odot}$, consistent with the episode of star formation that the LMC experienced 3–5 Gyr ago (Bertelli et al. 1992). They are characterized by a dual dust chemistry, being surrounded by a dust layer composed of carbonaceous particles, and a more external zone, harbouring silicates, alumina dust, and solid iron.

The presence of amorphous carbon, a featureless species, renders the SED of these objects significantly different from stars of similar obscuration and luminosity surrounded by O-bearing dust species only.

We believe that the dual dust chemistry originates from the transition to a C-rich photosphere during the final phase of life on the AGB. If this understanding is correct, we would expect these stars are C-rich, with a surface C/O not far in excess of unity. Considering the general low signal to noise of the IRS spectra, there are no apparently real or strong C_2H_2 absorptions at 7.5 and 13.7 μm in the stars proposed here; however, this is not surprising, as the optical depths of the carbon dust layers derived here, of the order of $\tau_1 \sim 0.3$ –0.7, make these features not clearly identifiable in the SED. Optical and/or NIR high-resolution spectroscopy would be valuable to confirm or disregard the present interpretation.

If confirmed, the results presented in this paper suggest that evolved stars with dual chemistry are expected to be found in galaxies where significant star formation in the epochs 1–4 Gyr ago occurred. Their identification will be possible in the context of the JWST mission, considering that they occupy specific regions in the various observational planes.

ACKNOWLEDGEMENTS

FDA and DAGH acknowledge support from the State Research Agency (AEI) of the Spanish Ministry of Science, Innovation and Universities (MCIU) and the European Regional Development Fund (FEDER) under grant AYA2017-88254-P.

REFERENCES

- Bernard-Salas J., Peeters E., Sloan G. C., Gutenkunst S., Matsuura M., Tielens A. G. G. M., Zijlstra A. A., Houck J. R., 2009, *ApJ*, 699, 1541
- Bertelli G., Mateo M., Chiosi C., Bressan A., 1992, *ApJ*, 388, 400
- Bunzel F., García-Hernández D. A., Engels D., Perea-Calderón J. V., García-Lario P., 2009, in Onaka T., White G. J., Nakagawa T., Yamamura I., eds, ASP Conf. Ser. Vol. 418, AKARI, a Light to Illuminate the Misty Universe. Astron. Soc. Pac., San Francisco, p. 431
- Cerrigone L., Hora J. L., Umana G., Trigilio C., 2009, *ApJ*, 703, 585
- Chan S. J., Kwok S., 1988, *ApJ*, 334, 362
- Dell’Aglì F., García-Hernández D. A., Rossi C., Ventura P., Di Criscienzo M., Schneider R., 2014, *MNRAS*, 441, 1115
- Dell’Aglì F., Ventura P., Schneider R., Di Criscienzo M., García-Hernández D. A., Rossi C., Brocato E., 2015a, *MNRAS*, 447, 2992
- Dell’Aglì F., García-Hernández D. A., Ventura P., Schneider R., Di Criscienzo M., Rossi C., 2015b, *MNRAS*, 454, 4235
- Feast M., 1999, *PASP*, 111, 775
- García-Hernández D. A., Górny S. K., 2014, *A&A*, 567, A12
- Groenewegen M. A. T., Sloan G. C., 2018, *A&A*, 609, A114
- Gutenkunst S., Bernard-Salas J., Pottasch S. R., Sloan G. C., Houck J. R., 2008, *ApJ*, 680, 1206
- Guzman-Ramirez L., Zijlstra A. A., Níchuimín R., Gesicki K., Lagadec E., Millar T. J., Woods P. M., 2011, *MNRAS*, 414, 1667
- Harris J., Zaritsky D., 2009, *AJ*, 138, 1243
- Jones O. C., Kemper F., Srinivasan S., McDonald I., Sloan G. C., Zijlstra A. A., 2014, *MNRAS*, 440, 631
- Jones O. C., Meixner M., Justtanont K., Glasse A., 2017, *ApJ*, 841, 15
- Kemper F. et al., 2010, *PASP*, 122, 683
- Lagadec E., Zijlstra A. A., 2008, *MNRAS*, 390, L59
- Little-Marenin I. R., 1986, *ApJ*, 307, L15
- Lloyd Evans T., 1990, *MNRAS*, 243, 336
- Marini E., Dell’Aglì F., Di Criscienzo M., Puccetti S., García-Hernández D. A., Mattsson L., Ventura P., 2019, *ApJ*, 871, L16
- Matsuura M., 2009, in Ueta T., Matsunaga N., Ita Y., eds, AGB stars and Related Phenomena, Conf. in Honor of Yoshikazu Nakada, Tokyo, Japan, p. 24,
- Meixner M. et al., 2006, *AJ*, 132, 2268
- Miller Bertolami M. M., 2016, *A&A*, 588, A25
- Molster F. J., Yamamura I., Waters L. B. F., Nyman L.-Å., Käufel H.-U., de Jong T., Loup C., 2001, *A&A*, 366, 923
- Perea-Calderón J. V., García-Hernández D. A., García-Lario P., Szczerba R., Bobrowsky M., 2009, *A&A*, 495, L5
- Schlegel D. J., Finkbeiner D. P., Davis M., 1998, *ApJ*, 500, 525
- Schneider R., Valiante R., Ventura P., dell’Aglì F., Di Criscienzo M., Hirashita H., Kemper F., 2014, *MNRAS*, 442, 1440
- Srinivasan S. et al., 2009, *AJ*, 137, 4810
- Stanghellini L., García-Lario P., García-Hernández D. A., Perea-Calderón J. V., Davies J. E., Manchado A., Villaver E., Shaw R. A., 2007, *ApJ*, 671, 1669
- Ventura P., Dell’Aglì F., Schneider R., Di Criscienzo M., Rossi C., La Franca F., Gallerani S., Valiante R., 2014, *MNRAS*, 439, 977
- Waelkens C., Van Winckel H., Waters L. B. F. M., Bakker E. J., 1996, *A&A*, 314, L17
- Willems F. J., de Jong T., 1986, *ApJ*, 309, L39
- Woods P. M. et al., 2011, *MNRAS*, 411, 1597
- Zaritsky D., Harris J., Thompson I. B., Grebel E. K., 2004, *AJ*, 128, 1606

This paper has been typeset from a $\text{\TeX}/\text{\LaTeX}$ file prepared by the author.